Journal of Luminescence 194 (2018) 401–406

Contents lists available at ScienceDirect

Journal of Luminescence

journal homepage: www.elsevier.com/locate/jlumin

Multicolour emission from surface crystallized Sm:Yb codoped spherulites rooted in borate matrix

Y. Dwivedi[a,*], S.B. Rai[b]

[a] Physics Department, National Institute of Technology, Kurukshetra, 136119 Haryana, India
[b] Physics Department, Banaras Hindu University, Varanasi 221005, Utter Pradesh, India

ARTICLE INFO

Keywords:
Spherulite
BaB_4O_7 nanocrystals
Surface crystallization
Lanthanide
Photoluminescence
Glass ceramic

ABSTRACT

This article reports on synthesis and spectroscopic characterizations of surface crystallized BaB_4O_7 nanocrystals doped with Sm and Sm:Yb rooted in borate glass which forms microsized 'Spherulites' while annealing for more than 06 h. Detailed nano and microstructural analysis were done using transmission, scanning electron microscopic and Polaroid optical microscope images; and XRD techniques which revealed the formation of cone - shaped BaB_4O_7 spherulites. Images under polarized light revealed birefringence property in tiny crystals rooted in glass- ceramic. A bright red dominated orange-red emission was observed under UV (266 nm) laser excitations. Emission intensity was found to be 08 multiple, in ceramics, then the glass counterpart. Formation of tiny crystals reinforces sharp emission peaks (FWHM ~ 1.6 nm) due to Sm^{3+} ions. We have confirmed formation of Yb^{2+}, Yb^{3+} and Sm^{3+} ionic species in the lattice which leads infrared cascade downconversion emissions spanning in the wide range of 380–1000 nm through involvement of intervalence charge transfer from Yb^{2+} to Yb^{3+} ions.

1. Introduction

Borate based glass-ceramic materials have vast industrial applications due to better thermal and chemical stabilities [1], high radiation-damage threshold [2], large band gaps [3], moderate phonon energies. Borate based lattices like crystals, ceramics etc. are known for excellent linear and non-linear optical properties [4]. Glass ceramics provide combined advantages of glass phase as well as tiny crystallites specifically when crystals are mostly developed close to the surface only. Crystallization near the surface develops a thick translucent surface while the central portion is remaining transparent. Crystallization near the surface occurs if the chemical composition of a glass is in non-stoichiometric ratio with respect to the corresponding crystal. In addition to the base composition of a glass, synthesis parameters and thermal history for crystallization play a crucial role to predict the ultimate crystalline phases and microstructures. Detailed discussion on surface crystallization in glass can be found from Ref. [5]. Highly non-equilibrium process involves in nucleation and crystal growth often leads to unique polycrystalline growth patterns that are broadly termed as 'spherulites'. Growth of Spherulites is expected due to the heterogeneities present in the sample. These heterogeneities affect the growth of new grains and associated branching of the growing crystal. Formation of spherulites are observed in variety of hosts including oxide and metallic glasses [6], mineral aggregates, volcanic rocks [7], polymers [8] etc. Formation of transparent $BaO–B_2O_3$ glass-ceramic was reported previously [9]. The most common crystalline phases in the Barium-borate oxide glassy matrix are BaB_2O_4, BaB_4O_7, BaB_8O_{13} etc. Among them monoclinic α-BaB_4O_7 crystal is well investigated in bulk, exhibits four [BO_3] triangular groups and four [BO_4] tetragonal groups sharing common vertices. The two crystallographically independent tetrahedral and triangular groups form a three dimensional $(B_4O_7)^{2-}$ network, which is repeated throughout the lattice structure.

Need of red colour emitting materials are in demand due to vast applications in various optical devices including LEDs, display devices etc. [10]. Several inorganic and organic materials are reported to emit bright red photoluminescence [11,12]. One of the lanthanide ions, Sm^{3+} is reported to yield strong emissions in visible region, leading to lasing, both in compact fiber and planar geometries. Sm ion used as a probe in variety of applications including optical memory, light guide, radiation dosimetry, pressure sensors, etc. [13–16]. Sm^{3+} ion exhibits both trivalent and divalent valence states. Its divalent valance state has been studied in different hosts [17,18]. Similar to Sm, Yb ion also exhibits two valence states which provide vast possibility of interaction among ionic species and hence colour tunability in spanning in UV-NIR regions and enhancement. Emission properties of Yb^{2+} ions have been less investigated which yields intense and broad yellow-green

* Corresponding author.
E-mail address: yashjidwivedi@gmail.com (Y. Dwivedi).

http://dx.doi.org/10.1016/j.jlumin.2017.10.042
Received 15 June 2017; Received in revised form 3 September 2017; Accepted 16 October 2017
Available online 17 October 2017

(535–560 nm) and blue emission [19,20]. However, even after considering all the peculiarities, interaction between Sm and Yb ions was not addressed well, in previous literature.

In the present work, we report formation of Sm and Yb codoped spherulites on the margin of borate glass matrix. We have reported bright red-orange emission spanning in the range of UV-IR on excitation with 266 nm laser photons due to the formation of Sm^{3+}, Yb^{2+} and Yb^{3+} ionic species and dominant interaction between them causing efficient radiative energy transfer from Yb^{2+} to Sm^{3+} ions and Intervalence charge transfer from Yb^{2+} to Yb^{3+} ion.

2. Experimental

The chemical compositions (69-x) H_3BO_3 + 25 BaF_2 + 5 LiF + 1 Sm_2O_3 + x Yb_2O_3 where x = 0, 0.5, 1, 1.5, and 2 mol% were used to prepare barium borate glass. All regents (H_3BO_3, BaF_2, LiF and Sm_2O_3) used was of high purity (~ 99.95%). All the glass samples were prepared using conventional melt and quench synthesis process. Firstly, all the ingredients were precisely weighed and mixed together for a half hour and annealed at 120 °C to remove moisture in powder. The well mixed starting materials were first melted at 1000 °C in a platinum crucible for 30 min in a computer controlled electric furnace. The molten mixture (free from air bubbles) was quenched by squeezing it into a rectangular steel cast preheated to 200 °C. The glasses were then gradually cooled to room temperature. The obtained glass samples were transparent and of good optical quality. The glass samples were cut and used without polishing for heating and optical measurements. The 'as prepared' glass samples were further processed through two steps thermal treatment resulting obtained glass-ceramic. Glasses were first annealed at 410 °C/2 h (heating rate 4.5 °C/min.) and thereafter at 520 °C and 620 °C (heating rate 10 °C/min.) for different time durations of 6, 8, 10 and 12 h. After annealing, tiny crystallites with the same stoichiometric composition of the as-prepared glass were precipitated inside samples. Samples annealed at 620 °C for heating time up to 10 h gradually become translucent due to the growth of larger crystalline size which effectively scattered ambient light and reduces transmittance and on further annealing it convert whole glass of milky white colour and opaque. Hereafter, glass ceramic samples heated at 620 °C are referring as GC6, GC8, GC10 and GC12.

Powder X-ray diffraction (XRD) measurements were carried out using Cu, K_α radiation from a RINT/DMAX 2200H/PC (Rigaku, Japan) machine having scan speed 2°/min. Data from International Centre for Diffraction Data sheet were used to identify the crystallized phases. Optical microscopy was performed with a Nikon™ Eclipse L150 microscope equipped with Nikon™ Coolpix 4.0 MP digital camera. Thickness of the crystallized layer was estimated from cross-sectional observation of the crystallized glass layer using the same microscope. SEM measurement was carried out on a JEOLTM Model JSM 5410 machine operated at 15 kV. Density of the samples was calculated by *Archimedes* principle while using hexane (density = 0.655 g/cm^3 at room temperature) as an immersion liquid. Density of glass ceramic samples was found to be 2.39, 2.40, 2.42, and 2.5 g/cm^3 for GC8, GC10, GC12, and GC15 samples, respectively, which is higher than as prepare glass 2.36 g/cm^3. The absorption spectra of the samples were recorded using Lambda 950 (Perkin Elmer, USA) in the 200–2300 nm range. The luminescence spectra of the samples were recorded on excitation with 266 nm radiation from a Nd:YAG laser. An iHR320 monochromator equipped with a photomultiplier tube (model no. 1424 M) was used to record the dispersed luminescence. The optical resolution of luminescence system was ~ 0.2 nm. Photoluminescence decay curves have been recorded using 266 nm pulsed radiation (~ 10 Hz, pulse width ~ 10 ns) of Nd:YAG laser. The collected signal was fed to 125 MHz digital oscilloscope and the decay curves were obtained for further analysis. Lifetimes of the radiative levels were estimated by fitting as exponential function to the recorded curves.

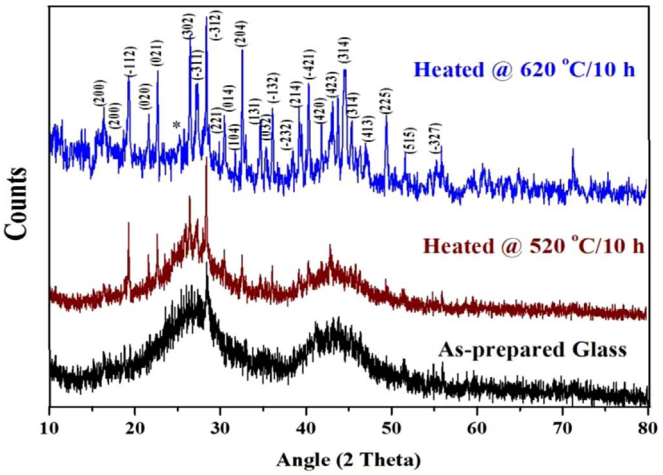

Fig. 1. X-ray diffraction patterns of as-prepared glass and annealed glass at 520 °C and 620 °C for 10 h. Peak marked with * is due to BaB_2O_4 crystals.

3. Results and discussion

3.1. Nanostructural characterizations

The prepared glass samples were annealed at fix temperature (570 °C) for different time durations and due to annealing, near the crystallization temperature, structural relaxation occurs to achieve most stable microstructure. Thermal treatments induce microstructural changes and precipitated phases which can be explored by X-ray diffraction patterns. Fig. 1 shows the diffraction patterns of glass and glass-ceramic samples. It can be seen that the as- prepared glass sample exhibits characteristic broad humps of the amorphous nature. However, the glassy phase fades away and several sharp peaks overlying the broad humps appear when annealed at 520 °C for 10 h. Further, annealing at 620 °C for 10 h reduced the glassy phase considerably and strengthens the sharp peaks which were indexed to monoclinic cell of the BaB_4O_7 crystals (JCPDS file no. 15-0860). Some of the small intensity peaks were identified as BaB_2O_4 (JCPDS: 38-0722) crystal, as a minor impurity phase, as well. Lattice parameters of BaB_4O_7 crystals are reported a = 10.58 Å, b = 8.19 Å, c = 13.04 Å, β = 105.1 in bulk while the value estimated from the diffraction pattern is slightly modified (a = 10.568 Å).

A comparison between the integrated diffraction intensity of the amorphous and the crystalline phase of the glass and GC10 has been made which reveals the crystallization of ~ 50–60% volume fraction of the glassy phase. The average crystallite size of the BaB_4O_7 crystals was calculated using the Debye-Scherrer's formula and the value was determined as ~ 250 nm.

We have analyzed the evolution of microstructure at different growth stages using optical fluorescence confocal microscope. Visual and optical microscopic examinations of the heat-treated glasses indicate that the crystallization started from the surface of the specimens. Microstructure precipitated in GC10 sample clearly shows the crystallization which preferably occurs near the surface (Fig. 2(A)). We have measured the thickness of crystallized layer ~ 1 mm. However, the thickness of crystallized layer increased further and colour of the sample become white in case of GC12 sample. In case of GC12 (Fig. 2(D)) big crystals of dimension 5 × 3 μm apparently cone shaped is clearly visible under microscope. It has been reported previously that the crystallization of glasses containing BaO and B_2O_3 preferably favour surface crystallization, and in some cases only the BaB_4O_7 crystals were nucleated [21]. Any non-stoichiometry in glass phase with respect to the crystal and surface defects preferably induced surface crystallization in glass.

Scanning electron microscope images (Fig. 2(B, C)) of the